




# Numerology-capable UAV-MEC for Future Generation Massive IoT Networks

Mohammad Arif Hossain , *Student Member, IEEE*, Abdullah Ridwan Hossain , *Student Member, IEEE*, and Nirwan Ansari , *Fellow, IEEE*

**Abstract**—This work proposes a dynamic numerology scheme assignment framework to provision mobile edge computing (MEC) for massive Internet-of-Things (IoT) networks via unmanned aerial vehicles (UAVs). IoT devices (IoTDs) usually lack computational power; thus, they offload their computational tasks to MEC servers. To enhance their battery lives, an optimal assignment of a numerology scheme to each IoTD is imperative; it also enhances the system spectral efficiency. In this work, we bring MEC services closer to a massive IoT network by deploying a UAV-MEC and allocate communication resources of the sub-6 GHz band dependent on the numerology schemes to each IoTD. We formulate a multi-objective optimization problem (MOOP) with two countering objectives to maximize the uplink spectral efficiency while minimizing the IoTDs' energy consumption. We solve a series of sequential sub-problems which are convex approximations of the MOOP and propose a novel algorithm to allocate computational resources, assign numerology schemes, and communication resources for each of the IoTDs. Our extensive simulation results validate the proposed aims herein.

**Index Terms**—Mobile Edge Computing, UAV, Internet of Things, Numerology, Spectral Efficiency, Energy Consumption.

## I. INTRODUCTION

The projected explosive growth of the volume of mobile and Internet-of-Things (IoT) devices is a grim forecast for the current mobile network infrastructure. Since IoT devices (IoTDs) need to maximize their battery lives, offloading their computational tasks to a mobile edge computing (MEC) server is a potential solution to minimize energy consumption. The sheer volume of tasks at MECs can quickly overwhelm the networks in their current state [1]–[3]. Network slicing, which is expected to be able to efficiently support heterogeneous applications such as enhanced mobile broadband (eMBB), ultra-reliable low latency communications (URLLC), and massive machine type communications (mMTC), is seen as one of the most promising technologies of future generation wireless networks (FGWN) such as 6G and beyond in addressing the aforementioned challenges [4]–[6].

Recently, it has been proposed to utilize unmanned aerial vehicles (UAVs) in conjunction with network slicing to better support the heterogeneous needs of the diverse services expected to be offered by FGWN. UAVs can enhance line-of-sight (LoS) communications and thus improve network

throughput and reliability. Non-line-of-sight (NLoS) communication with UAVs is also explored to similar ends [7], [8]. Besides, UAVs can readily leverage multiple-input and multiple-output (MIMO) and non-orthogonal multiple access (NOMA) alongside mmWave communications, all of which enhance the spectral efficiency and throughput significantly [9], [10]. More importantly, UAVs bring the last hop of a radio access network (RAN) even closer to the user-access end which is instrumental in shaving off network latency. Despite bringing the last mile of a RAN even closer, computing servers are still not near enough and require mobile connectivity for devices to offload tasks to them. In order to reduce the gap between such computing servers and IoT networks, we propose the deployment of a "flying edge-computing server" directly above the IoT networks.

In legacy networks, the resource allocation is fixed in terms of resource block (RB) bandwidth and duration [11], [12]. The lack of flexible RB bandwidths stands to be a major roadblock in the optimal provisioning for heterogeneous applications. In light of this, the 3GPP standardized the 5G numerology schemes to accommodate malleable RB bandwidths (and duration) [13], [14]. Incorporating the concept of numerology into UAV-aided MEC (hereon referred to as UAV-MEC) will prove to be instrumental in maximizing a device's uplink spectral efficiency and minimizing its energy consumption. Although the deployment of UAV-MEC may be hampered due to the battery capacity limitations, several research works have proposed feasible techniques enabling mid-air charging to maintain computational functionality [15], [16]. To the best of our knowledge, there has not been ample consideration for UAV-MEC with 5G numerology within the context of an IoT/mMTC network. In this work, UAVs, which are outfitted with MEC capabilities, allocate computing resources, numerology schemes, and communication resources over the sub-6 GHz band on a per-IoTD basis in an orthogonal frequency division multiple access (OFDMA) network. Consequently, we formulate a multi-objective mixed-integer non-linear programming (MINLP) problem to allocate computational resources for the offloaded tasks while maintaining their latency deadlines, maximize the uplink spectral efficiency and minimize the uplink energy consumption of IoTDs connected to the UAV network. In short, the contributions of this work can be briefly summarized as follows:

- We propose a novel numerology-capable UAV-MEC system to minimize the energy consumption of IoTDs in FGWN as well as to enhance the system spectral effi-

This work was supported in part by the U.S. National Science Foundation under Grant No. CNS-1814748.

The authors are with the Advanced Networking Laboratory, Department of Electrical and Computer Engineering, New Jersey Institute of Technology, Newark, NJ, 07102 USA (e-mail: mh624@njit.edu; arh24@njit.edu; nirwan.ansari@njit.edu).

ciency.

- We formulate a multi-objective optimization problem (MOOP), an MINLP problem, to jointly allocate computational and communication resources to IoTDs in order to maximize the spectral efficiency and minimize the energy consumption of IoTDs in the uplink direction.
- Our proposed numerology-capable UAV-MEC scheme allocates the sub-6 GHz numerology schemes at a highly granular level, i.e., on a per-IoTD basis, to fully maximize the tiling flexibility of resource assignments on the OFDMA resource grid such that it achieves the above-mentioned aims.
- Owing to the well-known NP-hardness of the MOOP, we transform the problem into a series of convex approximation sub-problems to tackle the MOOP problem by addressing one objective at a time.
- We propose the CONSTRUCTIVE (COmputing and CommuNication ReSource AllocaTion, NumeRology Scheme Association, and Uplink Power AlloCation for IoT Devices by UAV-MEC) algorithm to efficiently assign the computing resources for the IoT tasks prior to the numerology-enabled communication resources assignment. Subsequently, the numerology scheme for each device is assigned which is then followed by the allocation of the communication resources.
- We present our extensive simulation results to demonstrate different features of our proposed scheme.

The rest of the paper is organized as follows. Section II briefly reviews the recent related works while Section III presents the system model for this work. Section IV formulates the MINLP MOOP while Section V presents a series of sequential convex approximation sub-problems to solve the original MOOP. Section VI develops the CONSTRUCTIVE algorithm to solve the originally formulated optimization problem. Section VII presents the simulation results and detailed analyses. Finally, Section VIII offers concluding remarks and proposes areas of further research.

## II. RELATED WORKS

There have been extensive works already done in the field of UAV communications, especially related to network access and resource allocation. Mozaffari *et al.* [17] exploited a UAV to facilitate device-to-device communications. Al-Hourani *et al.* [18] derived the optimal UAV elevation which is dependent on the users' maximum pathloss thresholds to the radial coverage of the UAV. Alzenad *et al.* [19] maximized the number of served users by the UAV while minimizing the transmission power and satisfying the quality-of-service requirements of the users. Wang *et al.* [20] introduced challenges and research opportunities for multi-UAV-based heterogeneous flying ad hoc networks (FANET) architecture to improve the coverage and performance of UAVs. Liu and Ansari [21] proposed a UAV network access and resource allocation scheme to maximize the number of human portable/wearable machine type devices. Qian *et al.* [22] proposed to deploy a UAV to offload tasks from users to a MEC server by jointly optimizing the user association, UAV trajectory, and uplink power of the

users. Zhang and Ansari [23] proposed a latency-aware service provisioning mechanism for a UAV-aided MEC network. More recently, Yang *et al.* [24] studied multi-UAV-based MEC for IoT networks to tackle the computing challenges of heavy tasks of IoT nodes in UAVs. Hou *et al.* [25] proposed multi-UAV-based distributed fog computing architecture with latency and reliability constraints for computing to minimize the total required energy for computing and transmission of UAVs.

You *et al.* [26] explored optimizing resource allocation with numerology schemes and various frame types over the frequency and time domains, respectively. They studied the effects of numerology schemes on the throughput and latency of users. Weerasinghe *et al.* [27] studied grant-free resource allocations for mMTC traffic with dynamic time slot formats in a multi-numerology network. It also considered differing priorities for traffic within the time slots and developed Markov chain models to solve the allocation problems.

These works, however, have not considered multiple objectives for the holistic optimization of the network from the perspectives of spectral and energy efficiencies. Moreover, determining the optimal numerology scheme, especially more so on a per-user basis to establish an efficient assignment scheme, has yet to be solved. Such an optimization problem is valuable to solve considering that the maximization of system spectral efficiency and minimization of IoT energy consumption are in opposition to each other and are complicatedly related to the time domain as well. In this work, we seek to address these concerns.

## III. SYSTEM MODEL

We assume that a UAV-MEC is already optimally placed within a hotspot without loss of generality since the main focus of the work is on the designation of 5G numerology schemes and allocation of computational and communication resources. The optimal placement aims at maximizing the number of IoTDs which meet a minimum SINR threshold, i.e., to maintain connectivity to the UAV-MEC. The UAV-MEC of our proposed work utilizes OFDMA to transmit over the sub-6 GHz band. Furthermore, it is self-sufficient, i.e., it has the required computing power to carry out the resource allocation decisions as well as complete the tasks offloaded by IoTDs under its coverage area. We also assume that the UAV-MEC has radio frequency and/or optical charging capabilities to handle the required flight time, computational and communication burdens. It is, of course, capable of supporting the 5G numerology schemes for the sub-6 GHz band. We now proceed to outline the computational model utilized by the UAV-MEC followed by its communication model and describe the notations used throughout the paper in Table I.

Assume that within the hotspot, we have the following set of IoTDs denoted as  $\mathcal{U} = \{i | i = 1, \dots, |\mathcal{U}|\}$  where  $|\mathcal{U}|$  is the total number of IoTDs within the hotspot. Each IoTD offloads a single task to UAV-MEC (until it is completed) where the task is characterized by the parameters  $D_i$ ,  $Q_i$ , and  $L_i$  which refer to the latency deadline, required CPU cycles, and payload of the task, respectively. Note that the IoTDs have heterogeneous service requirements. We now denote  $C = \{j | j = 1, \dots, |C|\}$

as the set of virtualized computing resources (vCPUs) of the UAV-MEC with a total of  $|C|$  vCPUs and the capacity of vCPU  $j$  as  $F^j$  cycles per second. Denote  $\gamma_i^j$  as an indicator to assign vCPU  $j$  to IoTD  $i$ . Hence, the computational execution time for device  $i$  is

$$T_i^{MEC} = \frac{Q_i}{\sum_{j \in C} \gamma_i^j F^j}. \quad (1)$$

We utilize the sub-6 GHz band for massive IoT networks in this work because the utilization of mmWave bands under non-line-of-sight (NLoS) conditions is rather challenging. Resultantly, only numerology schemes 0, 1, and 2 are utilized by the UAV-MEC [28]. We denote a numerology scheme by  $x$  where  $x = \{0, 1, \dots, X\}$  and  $X \in \mathbb{Z}^+$ . The bandwidth of a frequency resource block (RB) of numerology scheme  $x$  is determined by  $180 * 2^x$ . We assume that the total available system bandwidth is  $W$  and the duration of a time slot of a numerology scheme  $x$  is  $T^{x,slot}$ . Besides, we consider a fixed number of radio frames in the time domain for the system bandwidth to serve a particular number of IoTDs by UAV-MEC. Denote the duration of a radio frame by  $T^{Fr}$  and there are  $N^{Fr}$  radio frames.

We denote the set of wireless resource blocks (RBs) belonging to numerology scheme  $x$  as  $\mathcal{M}^x = \{n | n = 1, \dots, |\mathcal{M}^x|\}$ .

TABLE I  
DESCRIPTION OF NOTATIONS

Notation	Description
$\gamma_i^j$	Assignment variable of vCPU $j$ for IoTD $i$
$\lambda_i^x$	Assignment variable of numerology scheme $x$ for IoTD $i$
$v_i^{n,x}$	Assignment variable of RB $n$ of scheme $x$ for IoTD $i$
$A$	Total number of available RBs for all numerology schemes
$N$	Total number of radio frames
$W$	Total available wireless system bandwidth
$B_i$	Allocated wireless bandwidth to IoTD $i$
$N_0$	Noise power spectral density
$D_i$	Latency deadline for the task of IoTD $i$
$L_i$	Payload of the task for the task of IoTD $i$
$Q_i$	Required CPU cycles for the task of IoTD $i$
$R_i$	Data rate of IoTD $i$
$E^{Eff}$	Energy efficiency of the system
$F^j$	CPU speed of vCPU $j$
$N^{Fr}$	Total number of radio frames
$P^{req}$	Total required wireless transmission power of all IoTDs
$P^{max}$	Total maximum UT power budget of all IoTDs
$S^{UT}$	Spectral efficiency for UT of the system
$T^{Fr}$	Duration of a radio frame
$T^{x,slot}$	Duration of a time-slot of numerology scheme $x$
$Z^x$	RB bandwidth for numerology scheme $x$
$P_i^{req}$	Required wireless transmission power of IoTD $i$
$P_i^{max}$	Maximum wireless transmission power of IoTD $i$
$p_i^{UT}$	Wireless transmission power of IoTD $i$
$g_i^{LoS}$	LoS channel gain of IoTD $i$
$g_i^{NLoS}$	NLoS channel gain of IoTD $i$
$P_{r_i}^{LoS}$	Probability of LoS channel of IoTD $i$
$P_{r_i}^{NLoS}$	Probability of NLoS channel of IoTD $i$
$R_i^{req}$	Required data rate of IoTD $i$
$E_i^{UT}$	Energy consumption for UT of IoTD $i$
$T_i^{UT}$	UT time of IoTD $i$
$T_i^{MEC}$	Computing time of the task of IoTD $i$ at UAV-MEC
$C$	Set of vCPUs of UAV-MEC
$\mathcal{U}$	Set of IoTDs within hotspot
$\mathcal{M}^x$	Set of RBs for numerology scheme $x$

The RB bandwidth varies in accordance with the numerology scheme and is denoted by  $Z^x$ . If  $\lambda_i^x$  represents the numerology scheme which is utilized by IoTD  $i$  and  $v_i^{n,x}$  reflects RB  $n \in \mathcal{M}^x$  of scheme  $x$  allocated to IoTD  $i$ , then the allocated wireless bandwidth to IoTD  $i$  is

$$B_i = \sum_{x=0}^X \lambda_i^x \sum_{n \in \mathcal{M}^x} v_i^{n,x} Z^x. \quad (2)$$

Therefore, we can express the data rate,  $R_i$ , of IoTD  $i$  by adopting the wireless throughput model presented in [15],

$$R_i = B_i \log_2 \left\{ 1 + \frac{p_i^{UT} g_i^{LoS}}{B_i N_0} \right\} \times Pr_i^{LoS} + B_i \log_2 \left\{ 1 + \frac{p_i^{UT} g_i^{NLoS}}{B_i N_0} \right\} \times (1 - Pr_i^{LoS}), \quad (3)$$

where  $p_i^{UT}$ ,  $g_i^{LoS}$ ,  $g_i^{NLoS}$ ,  $Pr_i^{LoS}$ ,  $P_{r_i}^{LoS}$ , and  $N_0$  denote utilized wireless transmission power, LoS channel gain, NLoS channel gain, probability of LoS channel, probability of NLoS channel for IoTD  $i$ , and noise power spectral density, respectively.

Now, uplink transmission (UT) time,  $T_i^{UT}$ , of IoTD  $i$ , energy consumption,  $E_i^{UT}$ , for UT of IoTD  $i$ , and spectral efficiency for UT of the system can be shown in (4), (5), and (6), respectively.

$$T_i^{UT} = \frac{L_i}{R_i} \quad (4)$$

$$E_i^{UT} = p_i^{UT} T_i^{UT} \quad (5)$$

$$S^{UT} = \frac{\sum_{i \in \mathcal{U}} R_i}{W} \quad (6)$$

#### IV. OPTIMIZATION PROBLEM

In accordance with the model presented in Section II, we formulate a MOOP for IoTDs to maximize the spectral efficiency while simultaneously minimizing the total wireless energy expenditure of the system in (7). The MOOP is as follows:

$$\begin{aligned} \mathbf{P0} : \quad & \max_{\gamma_i^j, \lambda_i^x, v_i^{n,x}, |\mathcal{M}^x|, p_i^{UT}} S^{UT} \\ & \min_{\gamma_i^j, \lambda_i^x, v_i^{n,x}, |\mathcal{M}^x|, p_i^{UT}} \sum_{i \in \mathcal{U}} E_i^{UT} \\ \text{s.t.} \quad & \text{C1} : \sum_{i \in \mathcal{U}} \gamma_i^j \leq 1, \quad \forall j \in C \\ & \text{C2} : \sum_{i \in \mathcal{U}} \sum_{j \in C} \gamma_i^j \leq |C| \\ & \text{C3} : T_i^{MEC} \leq D_i, \quad \forall i \in \mathcal{U} \\ & \text{C4} : \sum_{x=0}^X \lambda_i^x \leq 1, \quad \forall i \in \mathcal{U} \\ & \text{C5} : \sum_{i \in \mathcal{U}} \sum_{x=0}^X v_i^{n,x} \leq 1, \quad \forall n \in \mathcal{M}^x \\ & \text{C6} : \sum_{x=0}^X \sum_{n \in \mathcal{M}^x} v_i^{n,x} Z^x \leq |\mathcal{M}^x|, \quad \forall i \in \mathcal{U} \end{aligned} \quad (7)$$



$$\begin{aligned}
 \text{C7} : & \sum_{i \in \mathcal{U}} \sum_{x=0}^X \lambda_i^x \sum_{n \in \mathcal{M}^x} v_i^{n,x} Z^x \leq W \\
 \text{C8} : & \sum_{i \in \mathcal{U}} \sum_{x=0}^X \lambda_i^x \sum_{n \in \mathcal{M}^x} v_i^{n,x} T^{x,slot} \leq N^{fr} T^{fr} \\
 \text{C9} : & 0 \leq p_i^{UT} \leq P_i^{max}, \quad \forall i \in \mathcal{U} \\
 \text{C10} : & R_i \geq L_i / (D_i - T_i^{MEC}), \quad \forall i \in \mathcal{U} \\
 \text{C11} : & \gamma_i^j \in \{0, 1\}, \quad \forall i \in \mathcal{U}; j \in \mathcal{C} \\
 \text{C12} : & \lambda_i^x \in \{0, 1\}, \quad \forall i \in \mathcal{U}; x = 0, \dots, X \\
 \text{C13} : & v_i^{n,x} \in \{0, 1\}, \quad \forall i \in \mathcal{U}; n \in \mathcal{M}^x; x = 0, \dots, X
 \end{aligned}$$

The objective function of **P0** seeks to maximize the total spectral efficiency as well as to minimize the total energy consumed for UT of all IoTDs. In **P0**, **C1** enforces vCPU  $j$  to only be assigned to an IoTD. As it is assumed that IoTD  $i$  uploads only a single task at a time, "IoT D" and "task" are used synonymously from hereon. **C2** enforces that the total computing capacity possessed by the UAV-MEC is not violated. **C3** ensures that the task execution in the UAV-MEC is completed within the deadline  $D_i$  of IoTD  $i$ . **C4** restricts each IoTD to a single numerology scheme while that of **C5** enforces that each RB is assigned to a single IoTD. Furthermore, **C6** stipulates that the bandwidth allocated to the system is sufficient to serve each of the IoTDs by utilizing any of the numerology schemes. **C7** guarantees the total system bandwidth not to exceed by all the utilized numerology schemes while **C8** ensures the total time taken for UT not to violate the maximum time allotted which is indicated by the multiplication of the total number of radio frames  $N^{fr}$  and the duration of each radio frame  $T^{fr}$ . **C9** ensures the allocation of UT power for IoTDs up to a certain maximum power budget. **C10** stipulates that the data rate for UT should be sufficient to maintain the deadline requirement for IoTDs. This is because the deadline requirement considers the sum of the transmission ( $T_i^{UT}$ ) and computational ( $T_i^{MEC}$ ) times required. Finally, **C11** - **C13** enforce the binary nature of the utilized decision variables.

## V. SOLUTION TO MOOP

The MOOP is an MINLP problem due to the binary variables and constraints which relate to IoTDs' associations with numerology schemes, computational resources, and wireless resources. Therefore, the optimal solution of the proposed MOOP is intractable. Besides, the two objective functions of the MOOP incur additional complexities due to not only their dependencies on each other but their opposing aims and dependence on the time domain. Consequently, finding a near-optimal solution for the MOOP is challenging as well. We, however, can rewrite **P0** as **P1** in (8) by transforming the objective of maximizing the total system spectral efficiency  $S^{UT}$  into a throughput maximization objective as shown next (since the system bandwidth is merely a constant).

$$\begin{aligned}
 \text{P1} : & \max_{\gamma_i^j, \lambda_i^x, v_i^{n,x}, |\mathcal{M}^x|, p_i^{UT}} \sum_{i \in \mathcal{U}} R_i \\
 & \min_{\gamma_i^j, \lambda_i^x, v_i^{n,x}, |\mathcal{M}^x|, p_i^{UT}} \sum_{i \in \mathcal{U}} E_i^{UT}
 \end{aligned} \quad (8)$$

s.t. C1 – C13

Prior to simplifying the MOOP, we apply the  $\epsilon$ -constraint method to address the trade-off between the objective functions. This method entails keeping a single objective function only while transforming the other into a constraint bounded by  $\epsilon$ . This allows us to once again rewrite **P1** as **P2** in (9) below.

$$\text{P2} : \max_{\gamma_i^j, \lambda_i^x, v_i^{n,x}, |\mathcal{M}^x|, p_i^{UT}} \sum_{i \in \mathcal{U}} R_i \quad (9)$$

s.t. C1 – C13

$$\text{C14: } \sum_{i \in \mathcal{U}} E_i^{UT} \leq \epsilon$$

Here, **P2** becomes a single objective optimization problem with the constraint for total energy consumption of IoTDs bounded by  $\epsilon$ . Although  $E_i^{UT}$  depends on both  $p_i^{UT}$  and  $T_i^{UT}$ ,  $\epsilon$  depends mainly on  $p_i^{UT}$  of IoTDs because  $T_i^{UT}$  of IoTD  $i$  can be considered to be upper-bounded after the wireless resource allocations are carried out; recall that  $T_i^{UT}$  is inversely related to  $p_i^{UT}$ . We discuss the feasible solutions for the value of  $\epsilon$  later in this section.

As it is quite challenging to determine the optimal solutions to both the computational and communication resource allocations simultaneously as one depends on the other; therefore, one of the allocations needs to be solved prior to the other. Thus, we decompose **P2** into two sub-problems: **P2.A** and **P2.B** and solve them sequentially to obtain a sub-optimal solution for our MOOP. The former tackles the computing resource allocation problem while the latter solves the wireless resource allocation problem.

**Statement 1.** **P2.A** can be derived from **P2** to minimize MEC time  $T_i^{MEC} \forall i \in \mathcal{U}$  as this will allow further minimization of  $\sum_{i \in \mathcal{U}} E_i^{UT}$  by minimizing  $p_i^{UT} \forall i \in \mathcal{U}$  when the system bandwidth is kept fixed. We include the computing resource allocation constraints C1 - C3 and append two new constraints in C15 and C16 to replace the non-convex C11 but nevertheless enforce the binary nature of the concerned variable.

*Proof.* The total deadline to compute the task of IoTD  $i$  depends on both  $T_i^{MEC}$  and  $T_i^{UT}$ , and therefore, the minimization of  $T_i^{MEC}$  will accommodate the minimization of  $\sum_{i \in \mathcal{U}} E_i^{UT}$  by minimizing  $p_i^{UT} \forall i \in \mathcal{U}$  when the system bandwidth is kept unchanged as mentioned earlier. Observe that the computing resource allocation constraints are decoupled from those of the wireless resource allocation. Hence, we can formulate **P2.A** as shown in (10) to minimize the total MEC time of all IoTDs by considering C1 - C3 and C11. To address the non-convexity of C11, we replace it with two new constraints of C15 and C16.

$$\text{P2.A} : \min_{\gamma_i^j} \sum_{i \in \mathcal{U}} T_i^{MEC} \quad (10)$$

s.t. C1 – C13

$$\text{C15: } 0 \leq \gamma_i^j \leq 1, \quad \forall i \in \mathcal{U}; j \in \mathcal{C}$$

$$\text{C16: } \gamma_i^j - (\gamma_i^j)^2 \leq 0, \quad \forall i \in \mathcal{U}; j \in \mathcal{C}$$

**Theorem 1.** *P2.A' is equivalent to P2.A.*

*Proof.* To tackle the reverse-convex function in C16, we remove it as a constraint and factor it into the objective function of **P2.A'** via a multiplicative penalty function. Here,  $\phi$  is a sufficiently large constant value ( $\phi \gg 1$ ) which restricts the penalty function's value to either 0 or 1 whenever  $\gamma_i^j$  invalidates C16. Therefore, **P2.A'** can be expressed as follows in (11) and is indeed equivalent to **P2.A**.

$$\begin{aligned} \mathbf{P2.A}' : \quad & \min_{\gamma_i^j} \sum_{i \in \mathcal{U}} T_i^{MEC} + \phi \{\gamma_i^j - (\gamma_i^j)^2\} \quad (11) \\ \text{s.t.} \quad & \text{C2, C3, C15} \end{aligned}$$

**Lemma 1.** *P2.A' is a convex optimization problem.*

*Proof.* From (11), we observe that  $T_i^{MEC}$  is a function of  $Q_i$ ,  $F^j$ , and  $\gamma_i^j$ , where  $Q_i$  and  $F^j$  are given. The value of  $\gamma_i^j$  is continuous as per C15 and is thus convex. The penalty factor is a large value which forces the penalty function to be either 0 or 1 when C15 is violated. Consequently, the objective function of **P2.A'** is convex and it makes **P2.A'** a convex optimization problem.  $\square$

**Statement 2.** *Optimization problem P2.B can be formulated from P2 once  $T_i^{MEC}$  is determined from P2.A. P2.B deals with the user associations to numerology schemes, wireless resource and transmission power allocations, i.e, C4 - C10, C14, and the two pairs of additional constraints which address the binary nature of C12 and C13.*

*Proof.* Now, we can formulate **P2.B** as shown in (12) with the objective of maximizing  $\sum_{i \in \mathcal{U}} R_i$  where the constraints are related to numerology scheme assignment, wireless resource and UT power allocation as computing resource allocation is tackled in **P2.A** already. Similar to **P2.A**, we tackle the non-convexity of C12 and C13 by replacing them with C17 - C20 in **P2.B**.

$$\begin{aligned} \mathbf{P2.B} : \quad & \max_{\lambda_i^x, v_i^{n,x}, |\mathcal{M}^x|, p_i^{UT}} \sum_{i \in \mathcal{U}} R_i \quad (12) \\ \text{s.t.} \quad & \text{C6 - C10, C14} \\ & \text{C17: } 0 \leq \lambda_i^x \leq 1, \quad \forall i \in \mathcal{U}; x = 0, \dots, X \\ & \text{C18: } \lambda_i^x - (\lambda_i^x)^2 \leq 0, \quad \forall i \in \mathcal{U}; x = 0, \dots, X \\ & \text{C19: } 0 \leq v_i^{n,x} \leq 1, \quad \forall i \in \mathcal{U}; n \in \mathcal{M}^x; x = 0, \dots, X \\ & \text{C20: } v_i^{n,x} - (v_i^{n,x})^2 \leq 0, \quad \forall i \in \mathcal{U}; n \in \mathcal{M}^x; x = 0, \dots, X \end{aligned}$$

Similar to C16 of **P2.A**, C18 and C20 of **P2.B** are reverse-convex. Hence, we transform **P2.B** to **P2.B'** to tackle their reverse-convexity.  $\square$

**Theorem 2.** *P2.B' is equivalent to P2.B.*

*Proof.* In **P2.B'**, we transform the maximization objective into a minimization problem by taking the negative of  $R_i$ . Furthermore, we incorporate two penalty functions,  $\chi \{\lambda_i^x - (\lambda_i^x)^2\}$  and  $\psi \{v_i^{n,x} - (v_i^{n,x})^2\}$ , to tackle the reverse-convex C18 and

$\square$  C20. Here,  $\chi$  is a penalty factor (a sufficiently large value) to force the value of  $\chi \{\lambda_i^x - (\lambda_i^x)^2\}$  to be either 0 or 1 when C17 violates C18. Likewise, a similar statement can be made for  $\psi \{v_i^{n,x} - (v_i^{n,x})^2\}$ ; therefore, we can remove C18 and C20 from **P2.B** and use them as penalty functions to present an equivalent problem **P2.B'** in (13).

$$\begin{aligned} \mathbf{P2.B}' : \quad & \min_{\lambda_i^x, v_i^{n,x}, |\mathcal{M}^x|, p_i^{UT}} \left[ \sum_{i \in \mathcal{U}} -R_i + \chi \{\lambda_i^x - (\lambda_i^x)^2\} \right. \\ & \left. + \psi \{v_i^{n,x} - (v_i^{n,x})^2\} \right] \quad (13) \\ \text{s.t.} \quad & \text{C6 - C10, C14, C17, C19} \end{aligned}$$

Note that **P2.B'** is not a convex problem as  $E_i^{UT}$  in C14 is a function of both  $p_i^{UT}$  and  $T_i^{UT}$ . Minimizing the energy expenditure of an IoTD will inevitably result in the minimization of its throughput. Furthermore, lowering UT power increases the time it takes for UT. We observe that  $R_i$ ,  $p_i^{UT}$ ,  $T_i^{UT}$ , and  $E_i^{UT}$  are all coupled together, thus making **P2.B'** non-convex.  $\square$

**Statement 3.**  *$T_i^{UT}$  can be considered as upper-bounded after UT power and frequency RBs are allocated to IoTDs. Consequently, we can replace C14 with a new constraint to transform P2.B' into a convex problem.*

*Proof.* After the allocation of frequency RBs, UT time of IoTDs depends only on their UT power. Therefore,  $T_i^{UT}$  can be considered as to be upper-bounded when  $p_i^{UT}$  is estimated for IoTD  $i$ . As  $E_i^{UT}$  is a function of  $p_i^{UT}$  for IoTD  $i$ , we can replace C14 by a constraint for  $p_i^{UT}$  instead of  $E_i^{UT}$  (UT time is upper-bounded) with another bounded value  $\epsilon'$ . Hence, **P2.B'** can be expressed as follows:

$$\begin{aligned} \mathbf{P2.B}' : \quad & \min_{\lambda_i^x, v_i^{n,x}, |\mathcal{M}^x|, p_i^{UT}} \left[ \sum_{i \in \mathcal{U}} -R_i + \chi \{\lambda_i^x - (\lambda_i^x)^2\} \right. \\ & \left. + \psi \{v_i^{n,x} - (v_i^{n,x})^2\} \right] \quad (14) \\ \text{s.t.} \quad & \text{C6 - C10, C17, C19} \\ & \text{C21: } \sum_{i \in \mathcal{U}} p_i^{UT} \leq \epsilon' \end{aligned}$$

Here,  $\epsilon' = \sum_{i \in \mathcal{U}} \epsilon'_i$  and  $\epsilon'_i \forall i \in \mathcal{U}$  can be determined from data rate requirement and maximum available UT power of IoTDs. The required data rate of IoTD  $i$  (from C10) is

$$R_i^{req} = L_i / (D_i - T_i^{MEC}). \quad (15)$$

Let us denote  $P_i^{req}$  and  $P_i^{max}$  as required and maximum wireless transmission powers of IoTD  $i$ , respectively. Therefore, the upper and lower bounds of  $\epsilon'_i$  and  $\epsilon'$  can be determined as follows:

$$P_i^{req} \leq \epsilon'_i \leq P_i^{max} \quad \forall i \in \mathcal{U} \quad (16)$$

$$P^{req} \leq \epsilon' \leq P^{max} \quad (17)$$

$$P^{req} = \sum_{i \in \mathcal{U}} P_i^{req} \quad (18)$$

$$P^{max} = \sum_{i \in \mathcal{U}} P_i^{max} \quad (19)$$

$\square$

**Lemma 2.** *P2.B' is a convex optimization problem.*

*Proof.* The relaxation of  $\lambda_i^x$  and  $v_i^{n,x}$  into continuous values for **P2.B'** makes them and C6 - C8 convex. C9, C10, C17, and C19 are likewise convex.  $\epsilon'$  is a continuous value between  $\sum_{i \in \mathcal{U}} P_i^{req}$  and  $\sum_{i \in \mathcal{U}} P_i^{max}$ . Therefore, C21 is also convex.  $R_i$  is a well-known concave function, and thus  $-R_i$  is a convex function and so is **P2.B'** as a whole.  $\square$

**Statement 4.** *The optimal solution of **P2.B'** depends on  $\epsilon'$  as the value of the objective function of **P2.B'** varies with  $\epsilon'$ . We can establish a relationship between  $\epsilon'$  and  $P^{max}$  to obtain the optimal solution for **P2.B'** by satisfying (17).*

*Proof.* The optimal solution of **P2.B'** can vary based on the value of  $\epsilon'$ . The ultimate objective of this work is to maximize spectral efficiency and minimize energy consumption. Therefore, there can be several sub-optimal solutions based on the value of  $\epsilon'$  as there is a trade-off between the data rate and UT power. Hence, we consider the following cases:

If  $\epsilon' < P^{req}$  and  $\epsilon' > P^{max}$ , **P2.B'** will not have any feasible solution for the system as the minimum data rate requirement cannot be fulfilled and UT power budget can be exceeded for some IoT devices, respectively. If  $P^{req} \neq P^{max}$  and  $\epsilon' = P^{req}$ , **P2.B'** will achieve a system throughput with the optimal (minimal) UT power. However, the throughput is not optimal as the throughput can be increased by increasing the UT power. If  $P^{req} = P^{max}$  and  $\epsilon' = P^{req}$ , **P2.B'** will have a maximized system throughput with minimized UT power. In this case, the throughput is optimal because it cannot be increased by increasing the UT power. If  $P^{req} < \epsilon' < P^{max}$ , **P2.B'** will either achieve an optimal or sub-optimal solution for a maximized throughput with minimized UT power. If  $P^{req} \neq P^{max}$  and  $\epsilon' = P^{max}$ , **P2.B'** will have a maximum throughput for a specific UT power. The throughput is optimal but the total energy consumption is not.

Based on the above-mentioned cases, it is obvious that the value of  $\epsilon'$  needs to be chosen carefully. Now, we define a variable  $\eta$  where  $\eta \in [0, 1]$  to evaluate  $\epsilon'$  with respect to  $P^{req}$  and  $P^{max}$  in (20).

$$\epsilon' = P^{req} + \eta(P^{max} - P^{req}) \quad (20)$$

It is obvious that  $\epsilon' = P^{max}$  and  $\epsilon' = P^{req}$  when  $\eta = 1$  and  $\eta = 0$ , respectively. Therefore, we can define  $\eta$  by  $\eta \in (0, 1)$  when  $P^{req} \neq P^{max}$  and obtain the optimal solution for **P2.B'**.  $\square$

## VI. PROPOSED ALGORITHM

In this section, we present our proposed **CONSTRUCTIVE** algorithm (**C**omputing and **C**ommunication **R**esource **A**llocation, **N**umerology **S**cheme **A**ssociation, and **U**plink **P**ower **A**llocation to **I**oT **D**evice**s** for **U**AV-**M**EC). The very first step of **CONSTRUCTIVE** allocates vCPUs of the UAV-MEC to IoT devices by solving **P2.A'** to determine the optimal  $T_i^{MEC}$  for each IoT device  $i \in \mathcal{U}$  (lines 1-7). The next phase of **CONSTRUCTIVE** associates IoT devices to different numerology schemes, and allocates wireless RBs and uplink transmit power to all IoT devices in order to achieve the maximum data rate  $R_i \forall i \in \mathcal{U}$  that the network can support (lines 8-12). As our main objective is to maximize the uplink spectral efficiency and minimize the total UT energy consumption, we determine

### Algorithm 1: CONSTRUCTIVE Algorithm

---

**Input:**  $\phi, \chi, \psi, d_i, D_i, F^j, L_i, P_i^{max}, Q_i, C, \mathcal{U}$   
**Output:**  $\eta, \gamma_i^j, \lambda_i^x, v_i^{n,x}, p_i^{UT}, E_i^{UT}, S^{UT}, T_i^{MEC}$

- 1 Initialize iteration  $t = 0$  for MEC resource allocation.
- 2 **repeat**
- 3   Solve **P2.A'** to find  $\gamma_i^j(t)$  and  $T_i^{MEC}(t) \forall i \in \mathcal{U}$ .
- 4   Set  $t = t + 1$ .
- 5 **until** **P2.A'** converges i.e.,  $\sum_{i \in \mathcal{U}} T_i^{MEC} + \phi \{\gamma_i^j - (\gamma_i^j)^2\}$  reaches to its global minima by satisfying C2, C3, and C15.
- 6 Initialize iteration  $v = 0$  for bandwidth and transmit power allocation.
- 7 **repeat**
- 8   Solve **P2.B'** to determine  $\lambda_i^x(v), v_i^{n,x}(v), p_i^{UT}(v)$ , and  $R_i(v) \forall i \in \mathcal{U}$ .
- 9   Determine  $P^{req}(v)$  and  $P^{max}(v)$  by using Eqs. (18) and (19), respectively.
- 10   Determine  $\epsilon'(v)$  for  $\eta(v) \in (0, 1)$  by using Eq. (20).
- 11   Set  $v = v + 1$ .
- 12 **until** **P2.B'** converges, i.e.,  $[\sum_{i \in \mathcal{U}} -R_i + \chi \{\lambda_i^x - (\lambda_i^x)^2\} + \psi \{v_i^{n,x} - (v_i^{n,x})^2\}]$  reaches to its global minima by satisfying C6 - C10, C14, C17, C19.
- 13 Estimate  $T_i^{UT}, E_i^{UT} \forall i \in \mathcal{U}$ , and  $S_{UT}$  by using Eqs. (4), (5), and (6), respectively.
- 14 Estimate the optimal value of  $\eta$  to maximize Eq. (21).

---

$P^{req}$  which achieves the minimum data rate possible while still satisfying the latency requirement of the tasks to be executed in UAV-MEC. The next step estimates  $\eta$  from  $P^{req}$  and  $P^{max}$  to determine the value of  $\epsilon'$  which is needed to solve **P2.B'**. Then, the total uplink energy consumption  $\sum_{i \in \mathcal{U}} E_i^{UT}$  and uplink spectral efficiency  $S^{UT}$  are determined. However, the optimal value of  $\eta$ , which ultimately determines the optimal value of  $\epsilon'$ , is estimated by maximizing the system energy efficiency. The uplink energy efficiency of the system is defined as the ratio of the uplink throughput and total uplink energy consumption. If we denote the energy efficiency of the system by  $E^{Eff}$ , then  $E^{Eff}$  is:

$$E^{Eff} = \frac{S^{UT}}{\sum_{i \in \mathcal{U}} E_i^{UT}}. \quad (21)$$

Therefore, the MOOP can be solved by determining an optimal value of  $\eta$  which in turn maximizes the system's energy efficiency.

The complexity of **CONSTRUCTIVE** is primarily dictated by the complexity of its convex sub-problems. In general, the time complexity of solving a convex optimization problem by using the interior point primal dual method is  $O(\log \sqrt{N})$  where  $N$  denotes the size of the convex problem [4]. Therefore, the complexity of **P2.A'** is  $O(\log \sqrt{C|\mathcal{U}|})$  (lines 1-7) while that of **P2.B'** is  $O(\log \sqrt{AX|\mathcal{U}|})$  (lines 8-12). Here,  $A = \sum_{x=0}^X W/(180 * 2^x)$  determines the total number of available RBs over all the numerology schemes  $x$ . Note that we do not consider the number of iterations  $t$  and  $v$  here since the iterations do not increase the complexities of the



TABLE II  
SIMULATION PARAMETERS

Parameter	Value
Hotspot area	100×100 sq m
Required latency for IoTDs	400-500 ms
Data size of IoTDs	5000-7000 bits
Workload of IoTDs	0.1-0.5 Giga cycles
Number of vCPUs in UAV-MEC	256
Speed of vCPU	1 GHz
System bandwidth	10 MHz
Time duration of a radio frame	10 ms
Number of radio frames	1
Numerology schemes	0,1, and 2
Carrier frequency	2.4 GHz
Noise power spectral density	-174 dBm/Hz
Maximum UE transmit power	27 dBm
Environmental constants	9.6, 0.28
Average LoS attenuation	1 dB
Average NLoS attenuation	20 dB

convex optimization sub-problems in CONSTRUCTIVE. The total complexity of CONSTRUCTIVE can be expressed as  $O(\log \sqrt{|C||\mathcal{U}|} + \log \sqrt{AX|\mathcal{U}|})$ , which can be simplified as  $O(\log \sqrt{|C||\mathcal{U}|})$  when  $|C| \geq AX$  or as  $O(\log \sqrt{AX|\mathcal{U}|})$  when  $|C| < X$ . Therefore, CONSTRUCTIVE has a polynomial time complexity.

From the analysis, we find that the complexity of the CONSTRUCTIVE algorithm can be presented as  $O(\log \sqrt{N^2})$ . Here, we consider  $|C||\mathcal{U}|$  or  $A|\mathcal{U}|$  as  $N^2$  by neglecting  $X$  since  $X$  is a small number that represents a numerology scheme. Consequently, we find that the overall complexity of the proposed CONSTRUCTIVE algorithm can be expressed as  $O(\log N)$ .

## VII. SIMULATION RESULTS

In this section, we discuss our simulation results to validate CONSTRUCTIVE's performance. The simulation parameters are as shown in Table II. We also use 100 IoTDs for simulations when the number of IoTDs is kept fixed. Firstly, we compare the aggregate energy expenditure for Long Term Evolution (LTE) system where the RB bandwidth is fixed (180 kHz) and our proposed system (CONSTRUCTIVE). In Fig. 1, we observe that the energy expenditure of our scheme is significantly lower than that of the LTE scheme. Specifically, for 100 IoTDs, the energy consumption of CONSTRUCTIVE is 8000 mJ while that of LTE is approximately 9000 mJ. This is because the LTE scheme does not afford flexibility on the RB grid as that of the flexible numerology scheme of CONSTRUCTIVE. Recall that utilizing several schemes allows for a highly efficient tiling mechanism of RB assignments. Moreover, utilizing a higher scheme will allow for a shorter transmission time but more frequency bandwidth, decrease the transmission power over such and thus lower the overall energy consumption of an IoTD. Hence, under various IoT loads, CONSTRUCTIVE outperforms the traditional resource allocation scheme. Obviously, the more IoTDs in the network, the higher the aggregate energy expenditure will be. We should point out here that for smaller IoT networks, the energy expenditure difference is not too pronounced since both the CONSTRUCTIVE and LTE schemes can nearly minimize the

energy expenditure identically due to the lack of significant contention among IoTDs. However, as the size of the network increases, the gap between the two schemes becomes far more pronounced due to higher contention.

On the flip side, we assess the aggregate spectral efficiency of the same scenario. In Fig. 2, CONSTRUCTIVE greatly enhances the spectral efficiency because the higher RB bandwidths afford higher throughputs in a shorter period. Observing the performance improvement at a scale of 100 IoTDs, we see that CONSTRUCTIVE achieves a spectral efficiency of 5.6 bps/Hz while the LTE scheme has a mere 4 bps/Hz efficiency. We note that for smaller IoT networks, the spectral efficiency difference is not too pronounced since both the CONSTRUCTIVE and LTE schemes can nearly identically enhance the spectral efficiency due to the lack of significant contention among IoTDs. Furthermore, enhancing the spectral efficiency too much will require extra UT power leading to increased energy consumption. As the scale of the network increases, the gap between the two allocation schemes becomes far more pronounced due to higher contention, and thus, the devices in the LTE scheme must settle for fewer resources.

Similar to Fig. 1, we analyze the effect of total system bandwidths on the aggregate energy consumption and spectral efficiency of IoTDs in Fig. 2. We observe that the energy expenditures are significantly higher when the total system bandwidth is less (and vice versa); this is because IoTDs require higher UT powers to compensate for the limited bandwidth. Observably, the energy expenditure of CONSTRUCTIVE is always better than that of LTE regardless of bandwidth availability. Noticeably though, the performance gap becomes increasingly insignificant at higher system bandwidths as there tends to be over-provisioning. Therefore, CONSTRUCTIVE plays an extremely crucial role in allocating system bandwidth efficiently, more so in bandwidth-limited scenarios. On the other hand, the spectral efficiency improvement of CONSTRUCTIVE is very significant, especially at minimal system bandwidths (5 MHz). The effectiveness of CONSTRUCTIVE gradually declines with increasing system bandwidth since the throughput does not increase proportionally to the additional

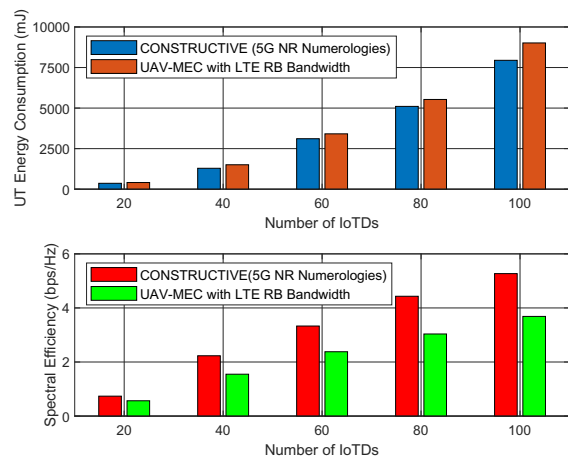


Fig. 1. Aggregate energy expenditure (top) and spectral efficiency (bottom) of the IoT network for different number of IoTDs.

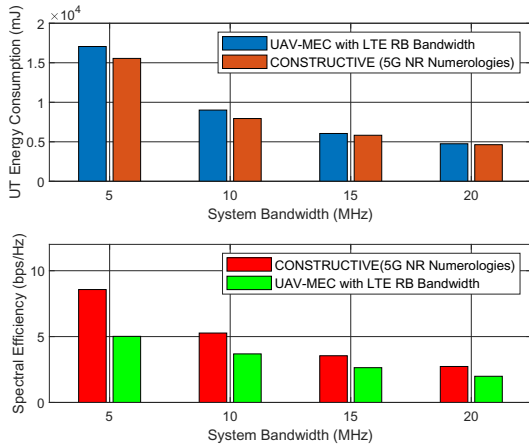


Fig. 2. Aggregate energy expenditure (top) and spectral efficiency (bottom) of the IoT network for various system bandwidths.

bandwidth. Despite the above, CONSTRUCTIVE outperforms the LTE scheme at all system bandwidth amounts.

Next, we investigate the network's performance with respect to power control, specifically as expressed in Eq. (17). Recall that  $P_i^{req}$  is the minimum transmission power required by IoTD  $i \in \mathcal{U}$  to satisfy its latency deadline whereas  $P_i^{max}$  is the maximum transmission power required by IoTD  $i \in \mathcal{U}$ . Therefore, there is a range of powers that an IoTD  $i \in \mathcal{U}$  can utilize to either maximize the spectral efficiency, minimize the power consumption, or balance between the two. In Fig. 3 we compare both the aggregate energy consumption and spectral efficiency of IoTDs when each IoTD  $i \in \mathcal{U}$  transmits at the minimum power (such that it satisfies its latency) vs. when it transmits at the maximum power. Generally, the spectral efficiency will be higher when transmitting at higher powers because the signal-to-noise ratio (SNR) is improved at higher numerology schemes. Nevertheless, the aggregated energy consumption of IoTDs increases significantly when they transmit at their maximum powers. Therefore, the system spectral efficiency can be improved with maximum transmission power but the overall system performance might be degraded due to the aggregate energy consumption of IoTDs.

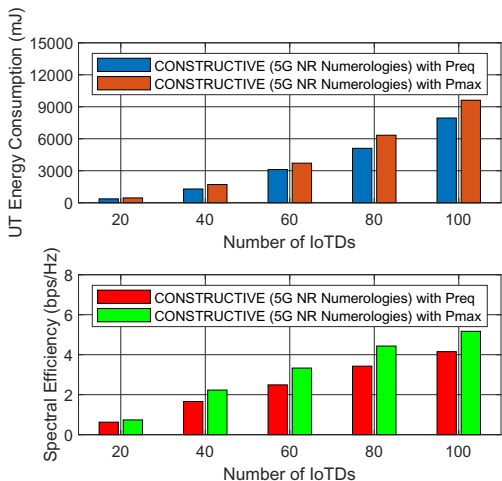


Fig. 3. Aggregate spectral efficiency of the massive-IoT network for  $P^{req}$  vs.  $P^{max}$ .

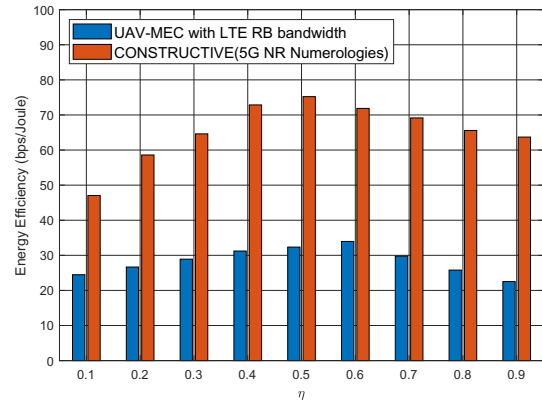


Fig. 4. Aggregate energy expenditure of the massive-IoT network for different  $\eta$  values.

Finally, in Fig. 4, we study the energy efficiency of the network which is defined as the throughput per unit of energy, i.e., bps/J. Recall that the MOOP seeks to maximize the network's spectral efficiency while simultaneously minimizing the energy consumption; essentially, this is maximizing the energy efficiency. The tuning parameter,  $\eta$ , shown in Eq. (20) helps us carefully choose the value of  $\epsilon'$  which is bounded between  $P^{req}$  and  $P^{max}$  as shown in Eq. (17). Note that the optimal  $\eta$  value that maximizes the ratio of spectral efficiency to energy expenditure is 0.6 for LTE, while that of CONSTRUCTIVE is 0.5. However, as  $\eta$  increases, much more UT power is utilized at the cost of minimal spectral efficiency improvement as IoTDs are operating in the bandwidth-limited regime.

## VIII. CONCLUSION

In this work, we have formulated a MOOP to jointly allocate computational and communication resources by utilizing 5G numerology to IoTDs to maximize spectral efficiency and minimize energy consumption for UT of a massive-IoT network supported by UAV-MEC. We decompose the MOOP into several sequential sub-problems to make it tractable and obtain a near-optimal solution. Most importantly, we apply the concept of 5G numerology and allocate the numerology schemes at a very granular level, on a per-device basis. We have then proposed the CONSTRUCTIVE algorithm to solve the MOOP and conducted extensive simulation results to validate our proposal. The advantages of our algorithm over the fixed allocation scheme are substantial, in that the spectral efficiencies achieved along with the reduced energy consumption for our CONSTRUCTIVE algorithm significantly surpass those of the baseline allocation scheme of LTE networks. Such advantages are even far more pronounced in larger-scale IoT networks. Future avenues of research should include machine learning-based MEC, especially for heterogeneous networks (HetNet) which are being supported by several UAVs simultaneously. Furthermore, the splitting of heterogeneous computational tasks among several UAV-MECs and the impact of utilizing mmWave frequencies in such scenarios should be studied in greater detail.



## REFERENCES

- [1] F. Guo *et al.*, "Enabling massive IoT toward 6G: A comprehensive survey," *IEEE Internet Things J.*, vol. 8, no. 15, pp. 11 891–11 915, 2021.
- [2] B. Qian *et al.*, "Multi-operator spectrum sharing for massive IoT coexisting in 5G/B5G wireless networks," *IEEE J. Sel. Areas Commun.*, vol. 39, no. 3, pp. 881–895, 2021.
- [3] X. Chen *et al.*, "Massive access for 5G and beyond," *IEEE J. Sel. Areas Commun.*, vol. 39, no. 3, pp. 615–637, 2021.
- [4] M. A. Hossain and N. Ansari, "Network slicing for NOMA-enabled edge computing," *IEEE Trans. Cloud Comput.*, pp. 1–1, 2021.
- [5] P. Yang *et al.*, "RAN slicing for massive IoT and bursty URLLC service multiplexing: Analysis and optimization," *IEEE Internet Things J.*, vol. 8, no. 18, pp. 14 258–14 275, 2021.
- [6] A. R. Hossain and N. Ansari, "Priority-based downlink wireless resource provisioning for radio access network slicing," *IEEE Trans. Veh. Technol.*, vol. 70, no. 9, pp. 9273–9281, 2021.
- [7] X. Pang *et al.*, "When UAV meets IRS: Expanding air-ground networks via passive reflection," *IEEE Wireless Commun.*, vol. 28, no. 5, pp. 164–170, 2021.
- [8] X. Zhang *et al.*, "IRS empowered UAV wireless communication with resource allocation, reflecting design and trajectory optimization," *IEEE Trans. Wireless Commun.*, pp. 1–1, 2022.
- [9] W. Feng *et al.*, "Joint 3D trajectory and power optimization for UAV-aided mmwave MIMO-NOMA networks," *IEEE Trans. Commun.*, vol. 69, no. 4, pp. 2346–2358, 2021.
- [10] X. Pang *et al.*, "Energy-efficient design for mmwave-enabled NOMA-UAV networks," *Sci. China Inf. Sci.*, vol. 64, no. 140303, Apr. 2021.
- [11] S. Parkvall, E. Dahlman, A. Furuskar, and M. Frenne, "NR: The new 5G radio access technology," *IEEE Commun. Stand. Mag.*, vol. 1, no. 4, pp. 24–30, 2017.
- [12] M. A. Hossain and N. Ansari, "Energy aware latency minimization for network slicing enabled edge computing," *IEEE Trans. Green Commun. Netw.*, vol. 5, no. 4, pp. 2150–2159, 2021.
- [13] S. Lien *et al.*, "5G new radio: Waveform, frame structure, multiple access, and initial access," *IEEE Commun. Mag.*, vol. 55, no. 6, pp. 64–71, 2017.
- [14] X. Liu *et al.*, "Peak-to-average power ratio analysis for OFDM-based mixed-numerology transmissions," *IEEE Trans. Veh. Technol.*, vol. 69, no. 2, pp. 1802–1812, 2020.
- [15] W. Liu, L. Zhang, and N. Ansari, "Laser charging enabled DBS placement for downlink communications," *IEEE Trans. Netw. Sci. Eng.*, vol. 8, no. 4, pp. 3009–3018, 2021.
- [16] W. Liu, S. Zhang, and N. Ansari, "Joint laser charging and DBS placement for drone-assisted edge computing," *IEEE Trans. Veh. Technol.*, vol. 71, no. 1, pp. 780–789, 2022.
- [17] M. Mozaffari, W. Saad, M. Bennis, and M. Debbah, "Unmanned aerial vehicle with underlaid device-to-device communications: Performance and tradeoffs," *IEEE Trans. Wireless Commun.*, vol. 15, no. 6, pp. 3949–3963, 2016.
- [18] A. Al-Hourani, S. Kandeepan, and S. Lardner, "Optimal LAP altitude for maximum coverage," *IEEE Wireless Commun. Lett.*, vol. 3, no. 6, pp. 569–572, 2014.
- [19] M. Alzenad, A. El-Keyi, F. Lagum, and H. Yanikomeroglu, "3-D placement of an unmanned aerial vehicle base station (UAV-BS) for energy-efficient maximal coverage," *IEEE Wireless Commun. Lett.*, vol. 6, no. 4, pp. 434–437, 2017.
- [20] J. Wang *et al.*, "Taking drones to the next level: Cooperative distributed unmanned-aerial-vehicular networks for small and mini drones," *IEEE Veh. Technol. Mag.*, vol. 12, no. 3, pp. 73–82, 2017.
- [21] X. Liu and N. Ansari, "Resource allocation in UAV-assisted M2M communications for disaster rescue," *IEEE Wireless Commun. Lett.*, vol. 8, no. 2, pp. 580–583, 2019.
- [22] Y. Qian *et al.*, "User association and path planning for UAV-aided mobile edge computing with energy restriction," *IEEE Wireless Commun. Lett.*, vol. 8, no. 5, pp. 1312–1315, 2019.
- [23] L. Zhang and N. Ansari, "Latency-aware IoT service provisioning in UAV-aided mobile-edge computing networks," *IEEE Internet Things J.*, vol. 7, no. 10, pp. 10 573–10 580, 2020.
- [24] L. Yang *et al.*, "Multi-UAV-enabled load-balance mobile-edge computing for iot networks," *IEEE Internet Things J.*, vol. 7, no. 8, pp. 6898–6908, 2020.
- [25] X. Hou *et al.*, "Distributed fog computing for latency and reliability guaranteed swarm of drones," *IEEE Access*, vol. 8, pp. 7117–7130, 2020.
- [26] L. You, Q. Liao, N. Pappas, and D. Yuan, "Resource optimization with flexible numerology and frame structure for heterogeneous services," *IEEE Commun. Lett.*, vol. 22, no. 12, pp. 2579–2582, 2018.
- [27] T. N. Weerasinghe, V. Casares-Giner, I. A. M. Balapuwaduge, and F. Y. Li, "Priority enabled grant-free access with dynamic slot allocation for heterogeneous mMTC traffic in 5G NR networks," *IEEE Trans. Commun.*, vol. 69, no. 5, pp. 3192–3206, 2021.
- [28] *5G; NR; Physical channels and modulation, 3GPP TS 38.211 version 15.2.0 Release 15*, 3GPP, 2018.